Computers and Structures 147 (2015) 26–35

Contents lists available at ScienceDirect

Computers and Structures

journal homepage: www.elsevier.com/locate/compstruc

Spectrum-compatible accelerograms with harmonic wavelets

Domenico Cecini, Alessandro Palmeri *

School of Civil and Building Engineering, Loughborough University, Sir Frank Gibb Building, Loughborough LE11 3TU, England, United Kingdom

ARTICLE INFO

Article history:
Accepted 9 October 2014
Available online 31 October 2014

Keywords:
Artificial accelerograms
Earthquake engineering
Harmonic wavelet transform (HWT)
Signal processing
Spectrum-compatible accelerograms

ABSTRACT

Modern building codes allow the analysis and design of earthquake-resistant structures with recorded and/or generated accelerograms, provided that they are compatible with the elastic design spectrum. The problem then arises to generate spectrum-compliant accelerograms with realistic non-stationary characteristics, which in turn may play an important role in the non-linear seismic response. In this paper, an iterative procedure based on the harmonic wavelet transform is proposed to match the target spectrum through deterministic corrections to a recorded accelerogram, localised both in time and frequency. Numerical examples demonstrate the performance of this approach, which can be effectively used in the design practice.

1. Introduction

Building codes conventionally define the seismic action through the elastic design spectrum (EDS), which is a way to represent synthetically the seismic hazard at a given site. Furthermore, the response spectrum analysis is widely recognised as the reference method for designing ordinary earthquake-resistant structures. In order to achieve a better understanding of the structural and non-structural performance under seismic forces, however, the time-history analysis is preferable. This method of analysis is particularly useful for non-conventional buildings, e.g. when the inelastic behaviour of some structural components (including isolators and dampers) must be accurately modelled, and cannot be simply accounted for by modifying the ordinates of the design spectrum with the ductility-dependent behaviour factor.

One of the key issues while carrying out the time-history analysis is the appropriate selection of the seismic input (e.g. Ref. [1]). International codes allow using both natural (i.e. recorded) and artificial (i.e. generated) time histories of ground acceleration and, besides generic prescriptions of being representative of the site hazard from a seismological point of view, their on-average spectrum-compatibility is required. That is, if the elastic response spectrum (ERS) is computed for each accelerogram of the selected suite, the mean value of the spectral ordinates for the periods of vibration within the rage of interest must satisfy the compatibility conditions with the corresponding ordinates of the EDS. As a consequence, if this suite is used to run linear-elastic time-history analyses, the discrepancy between the average seismic response so obtained and the EDS prescribed by the code will be small enough to be acceptable for design purposes.

In this context, the direct use of natural accelerograms is an attractive option and nowadays, with few exceptions of very soft soils in areas of high seismicity, numerous records are available. Unfortunately, the need to generate artificial ground motions still arises from the difficulty to form groups of motions with reasonable scatter around the target spectrum. These artificial records can be either simulated signals or recorded accelerograms modified to cope with the code prescriptions. Matching the EDS, however, is not a trivial task, mainly because the EDS given by seismic codes is a conventional and indirect representation of the expected ground shaking at a given site under some conventional design scenarios (i.e. for given return period and soil conditions), while an accelerogram provides a direct and full representation of the seismic action for a single event.

Importantly, the mapping between ERS and accelerograms is not bijective, as accelerograms provide richer information. Indeed, intensity, frequency content and duration of the ground shaking jointly contribute to build the ERS, but it is not possible to find them back individually. As a matter of fact, while a unique ERS can be computed from an accelerogram, a number of diverse accelerograms can be associated to (i.e. are compatible with) a target EDS. It follows that some of the above quantities must be specified to obtain the sought spectrum-compatible accelerograms (e.g. overall duration and energy content). In other words, the richer information allowed by the direct use of accelerograms (which is what makes worthwhile a time-history analysis for non-linear

* Corresponding author.
E-mail addresses: A.Palmeri@lboro.ac.uk, Dynamics.Structures@gmail.com (A. Palmeri).

http://dx.doi.org/10.1016/j.compstruc.2014.10.013
0045-7949/

structures, even if computationally more demanding) must be provided apart from the EDS offered by the seismic code.

Two alternative strategies can be pursued in this respect, as the additional information required to customise the generated accelerograms may be based either on the use of prediction laws (e.g. [2,3]), derived from seismological and geotechnical data, or on recorded ground motions (e.g. [4–9]). In both cases, the compatibility with the EDS is achieved while retaining some direct or indirect information on the expected non-stationary features in terms of amplitude and frequency content of the seismic action.

As far as the simulation of accelerograms is concerned, a number of different methods are available in the literature (for a review, see Refs. [10–12]), the vast majority of them being stochastic, i.e. they gain a certain level of abstraction from the underlying physical phenomenon. That is, the actual seismic genesis is not considered, and ground motion signals are mathematically handled as samples of a stationary or non-stationary random process [13–15,2,3,9]. Nonetheless, accelerograms generated in this way may not be ideal for some applications, especially for geotechnical systems (e.g. the Italian building code published in 2008 [16] explicitly bans their use for such applications) and for analyses where the energy content plays a crucial role [17,18].

In this framework, signal processing comes helpful to analyse, generate and manipulate accelerograms to be employed for different applications of earthquake engineering. A common practice is to use the Fourier transform (FT) to look at the recorded/generated signals in the frequency domain, where the distribution of the seismic energy at different frequencies becomes apparent. On the other hand, many studies (e.g. [19,20]) have shown the importance of modelling the temporal non-stationarity in the frequency content of the ground motion to properly assess the response of softening non-linear structures, and in this respect the accelerograms' non-stationary characteristics can be easily analysed in the time domain.

As a matter of fact, time and frequency domains are in a kind of dualism because they are capable of highlighting some relevant features of the signal, while hiding some others. Joint time–frequency signal representations can be therefore deemed as a powerful strategy to analyse the evolutionary frequency content of accelerograms, and getting the best from the two domains. Among them, the wavelet analysis (e.g. [21,22]) is a very promising tool, as it exploits localised functions (wavelets) instead of ever-lasting harmonics as a base to decompose a signal. The harmonic wavelet transform (HWT) enjoys the additional advantage of overcoming the limitations of the classical FT without losing a meaningful engineering interpretation in terms frequency content.

Further extending some preliminary results presented in [23], a novel HWT-based approach is proposed to generate a set of spectrum-compatible accelerograms, which allow satisfying the compatibility conditions with a target EDS starting from a parent accelerogram, while retaining the bulk of its non-stationary characteristics in terms of amplitude and frequency. This paper specifically addresses the problem of modifying deterministically a parent accelerogram in order to satisfy the compatibility requirements, while a second paper will be devoted in the future to the stochastic generation of an arbitrary number of time histories embedding the desired joint time–frequency properties of the spectrum-compatible signal, and to elucidate the optimal compromise between the two domains. The potential of the HWT in these two applications (deterministic correction and stochastic generation) has been partially shown in Ref. [23], and an additional effort has been done now in order to improve the required algorithms, facilitate the implementation and quantify their performance, also in comparison with previous research of other investigators.

This paper focuses on the problem of the deterministic correction and the main novelty lies in the fact that (to the best of the authors' knowledge) for the first time in the literature two complementary earthquake spectra (in terms of peak pseudo-acceleration, S_{PA}, and time instant at which such peak is attained, S_{ToM}) are jointly considered to calculate the corrective term in each iteration (allowing a simultaneous localisation of the deterministic corrections in both time and frequency domains). Indeed, although other applications of harmonic and non-harmonic wavelets can be found in the technical literature, the performance of existing methods are not completely satisfactory, as they do not take full advantage of their joint time–frequency localisation capabilities. In the method proposed by Mukherjee and Gupta [4], for instance, the Littlewood-Paley (L-P) basis of orthogonal wavelets (e.g. [24]) is used to decompose a recorded accelerogram into a finite number N of sub-signals with non-overlapping frequency bands, and then each sub-signals is iteratively scaled to match the target EDS. In their procedure, however, the sub-signals are uniformly scaled for the whole duration of the recorded accelerogram (i.e., the localisation is not exploited in the time domain), and therefore more energy is added than is strictly necessary. A similar matching scheme has been recently adopted by Giaralis and Spanos [15] as a way of post-processing the non-stationary samples generated from an analytically-defined uniformly-modulated (i.e. quasi-stationary) evolutionary power spectral density (PSD) function. Suárez and Montejo [5] have carried out the iterative spectral matching of a recorded accelerogram with a new family of wavelets, based on the impulse response function of an underdamped single-degree-of-freedom (SDoF) linear oscillator. Although the compatibility with the EDS is achieved, in all the results presented in their paper the amplitude of the corrective term is of the same order as the peak ground acceleration of the recorded signal (if not significantly higher), and such heavy adjustments reduces the practical advantages of their procedure in comparison with a direct stochastic generation. Aimed at overcoming such shortcomings, the proposed HWT-based matching scheme fully exploits the wavelets' localisation capabilities in both time and frequency domain, and in this way reduces the additional energy required to reach the spectral compatibility.

2. Harmonic wavelet analysis

The wavelet analysis consists of projecting a given signal on a convenient set of functions, called wavelets, which can be generated by scaling and shifting a mother wavelet [21]. In the continuous wavelet transform, the coefficient $a_{u,s}$ at scale s and position u of the signal $f(t)$ is given by:

$$a_{u,s} = \int_{-\infty}^{+\infty} f(t)\,\overline{\psi_{u,s}}(t)\,\mathrm{d}t, \tag{1}$$

where the over-bar denotes the complex conjugate, while:

$$\psi_{u,s}(t) = \frac{1}{\sqrt{s}}\,\psi\left(\frac{t-u}{s}\right) \tag{2}$$

is the mother wavelet $\psi(t)$ scaled by the parameter $s \in \mathbb{R}^+$ (controlling the frequency distribution) and shifted by the parameter $u \in \mathbb{R}$ (localising the function at around the time instant $t = u$). The inverse continuous wavelet transform is given by:

$$f(t) = \frac{1}{C}\int_{-\infty}^{+\infty}\int_{0}^{+\infty} \frac{1}{s^2}\,a_{u,s}\,\psi_{u,s}(t)\,\mathrm{d}s\,\mathrm{d}u, \tag{3}$$

in which C is simply a normalisation constant.

Unlike a harmonic wave, which is an ever-lasting periodic function, a wavelet is a decaying function, and this feature enables the localisation in time domain. Families of wavelets can be conveniently generated in a way to form an orthogonal basis, so that the wavelet transform is bijective, giving a unique representation

for any signal. This is the case of the harmonic wavelets proposed by Newland [25,26], which are complex-valued functions with a rectangular box-shaped FT:

$$\Psi(\omega) = \mathrm{FT}\langle\psi(t)\rangle = \frac{1}{2\pi}\int_{-\infty}^{+\infty}\psi(t)\,\mathrm{e}^{-\mathrm{i}\,2\pi\omega t}\,\mathrm{d}t = \frac{\mathrm{sgn}(4\pi-\omega)-\mathrm{sgn}(2\pi-\omega)}{4\pi}, \tag{4}$$

where the symbol $\mathrm{i}=\sqrt{-1}$ stands for the imaginary unit and the function $\mathrm{sgn}(\cdot)$ gives the sign of the real-valued quantity within parentheses, while the corresponding mother wavelet in the time domain is:

$$\psi(t) = \mathrm{FT}^{-1}\langle\Psi(\omega)\rangle = \int_{-\infty}^{+\infty}\Psi(\omega)\,\mathrm{e}^{\mathrm{i}\,2\pi\omega t}\,\mathrm{d}\omega = \frac{\mathrm{e}^{\mathrm{i}\,4\pi t}-\mathrm{e}^{\mathrm{i}\,2\pi t}}{\mathrm{i}\,2\pi t}. \tag{5}$$

It should be noted here that Eqs. (4) and (5) refer, without loss of generality, to the case of a signal of unitary time length, i.e. $0\leqslant t<1$, and therefore meaningful energy content for $\omega\geqslant 2\pi$. Moreover, among all the possible choices, the operators $\mathrm{FT}\langle\cdot\rangle$ and $\mathrm{FT}^{-1}\langle\cdot\rangle$ have been defined in order to have a unitary area for the graph of the real-valued function $\Psi(\omega)$, which indeed takes a constant value of $1/(2\pi)$ over the interval $[2\pi,4\pi[$, and zero outside (see the first rectangular block depicted within Fig. 1(a)).

The first discrete scheme proposed by Newland [25] to generate the whole family of orthogonal wavelets from the mother one is called dyadic, and can be derived by letting $s=2^{-j}, u=2^{-j}k$, namely by changing the argument in Eq. (5) from t to $(2^j t-k)$:

$$\hat{\psi}_{j,k}(t) = \psi_{2^{-j}k,2^{-j}}(t) = \psi\left(2^j t-k\right), \tag{6}$$

where j and k are integers, and the hat denotes the use of a discrete wavelet transform. By doing this, the shape of the wavelet is not changed, but its horizontal scale is compressed by the factor 2^j, being $j\geqslant 0$ the level of the wavelet, while its position is translated by k units at the new scale. Fig. 1(a) shows that, following Newland's dyadic scheme, the Fourier transform of the generic wavelet at the jth level occupies the frequency band from $2\pi 2^j$ to $4\pi 2^j$. The HWT coefficients can be obtained by substituting Eq. (6) into Eq. (1), and the expansion (reconstruction) formula for a real-valued signal $f(t)$ can be expressed as:

$$f(t) = 2\,\mathrm{Re}\left\{\sum_j\sum_{k=0}^{2^j}\hat{a}_{j,k}\,\hat{\psi}_{j,k}(t)\right\}, \tag{7}$$

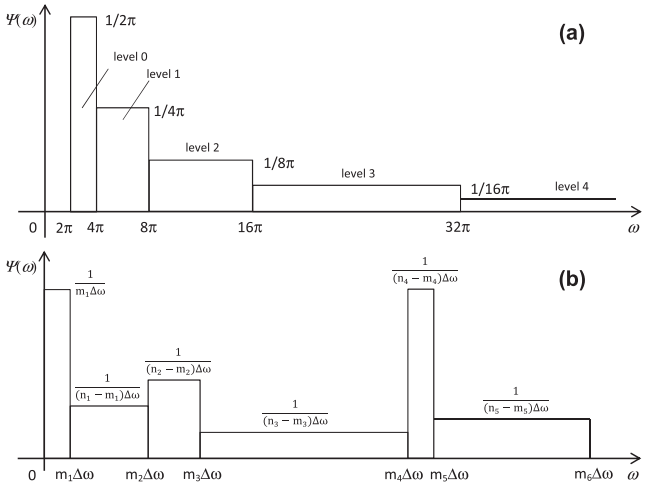

Fig. 1. Representation in the frequency domain: (a) dyadic scheme; (b) an example of generalised scheme for harmonic wavelet base with non-overlapping intervals ($n_i = m_{i-1}$) of arbitrary bandwidth (adapted from Newland [26]).

where the function $\mathrm{Re}\{\cdot\}$ gives the real part of the argument within curly brackets, while the first summation is intended over all j indexes.

The second scheme proposed by Newland [26] leads to the generalised HWT. Instead of splitting the frequency axis into bands of increasing width $B=\pi 2^{j+1}$, the whole set of band wavelets is generated by:

$$\hat{\psi}_{\{m,n\}}(t) = \frac{\mathrm{e}^{\mathrm{i}\,2n\pi t}-\mathrm{e}^{\mathrm{i}\,2m\pi t}}{\mathrm{i}\,2(n-m)\pi t}, \tag{8}$$

which in the frequency domain corresponds to a real-valued rectangular box function with a height of $1/[2(n-m)\pi]$ over the interval $[2m\pi,2n\pi[$:

$$\Psi_{\{m,n\}}(\omega) = \mathrm{FT}\left\langle\psi_{\{m,n\}}(t)\right\rangle = \frac{\mathrm{sgn}(2n\pi-\omega)-\mathrm{sgn}(2m\pi-\omega)}{4(n-m)\pi}. \tag{9}$$

Interestingly, if we put $m=2^j$ and $n=2^{j+1}$, we obtain the dyadic scheme as a particular case of the generalised HWT. The translation of the wavelet by a time step $k/(n-m)$ is then achieved by:

$$\hat{\psi}_{\{m,n\},k}(t) = \frac{\mathrm{e}^{\mathrm{i}\,2n\pi\left(t-\frac{k}{n-m}\right)}-\mathrm{e}^{\mathrm{i}\,2m\pi\left(t-\frac{k}{n-m}\right)}}{\mathrm{i}\,2(n-m)\pi\left(t-\frac{k}{n-m}\right)} = \hat{\psi}_{\{m,n\}}\left(t-\frac{k}{n-m}\right), \tag{10}$$

and in the frequency domain corresponds to:

$$\hat{\Psi}_{\{m,n\},k}(\omega) = \mathrm{FT}\left\langle\hat{\psi}_{\{m,n\}}(t)\right\rangle\exp\left(-\mathrm{i}\,\frac{k}{n-m}\,\omega\right). \tag{11}$$

For the real-valued signal $f(t)$, the reconstruction formula is readily written (like Eq. (7)) as:

$$f(t) = 2\,\mathrm{Re}\left\{\sum_{\{m,n\}}\sum_{k=0}^{n-m}\hat{a}_{\{m,n\},k}\;\hat{\psi}_{\{m,n\},k}(t)\right\}, \tag{12}$$

where the first summation is intended over all the $\{m,n\}$ pairs. According to Newland [26], with this generalised scheme we can no longer talk about wavelet level j, while the notation $\{m,n\}$ shall now be used to denote a wavelet occupying the band of circular frequencies from $2m\pi$ to $2n\pi$, where $n>m$, as shown within Fig. 1(b). In order to form a complete set of wavelets, adjacent levels must have a box-shaped FT, touching each other in the frequency domain but not overlapping, so that all values of ω are included and no one is taken twice. Apart from this, there are no further rules to choose the $\{m,n\}$ pairs and hence divide the frequency axis. Importantly, while the unique scaling factor of the dyadic scheme relate the bandwidth and the central frequency of each level, i.e. they are not independent, the incorporation of an additional parameter in the generalised scheme provides more flexibility in the treatment of the signal.

Aimed at highlighting the key advantage of the HWT in comparison with the traditional FT, and therefore justify the exploitation of the HWT in this study, Fig. 2 offers the representation in both a joint time–frequency domain (top row) and in the time domain only (bottom row) of a periodic harmonic wave (left column) and of a fading harmonic wavelet (right column). It can be seen that the harmonic wave is perfectly localised in the frequency domain (Fig. 2(a)), that is the energy is fully concentrated at the frequency ω_j, while its periodic nature does not allow any localisation in the time domain (Fig. 2(c)). By contrast, the harmonic wavelet is well localised around the time instant $t=t_k$ (Fig. 2(d)), fading as $(t-t_k)^{-1}$ (see Eqs. (5)), but the energy is spread over the frequency interval from ω_m to ω_n (Fig. 2(b)).

These differences between harmonic waves and wavelets have important implications when a certain component has to be extracted from given signal, as illustrated by Fig. 3 for the case of

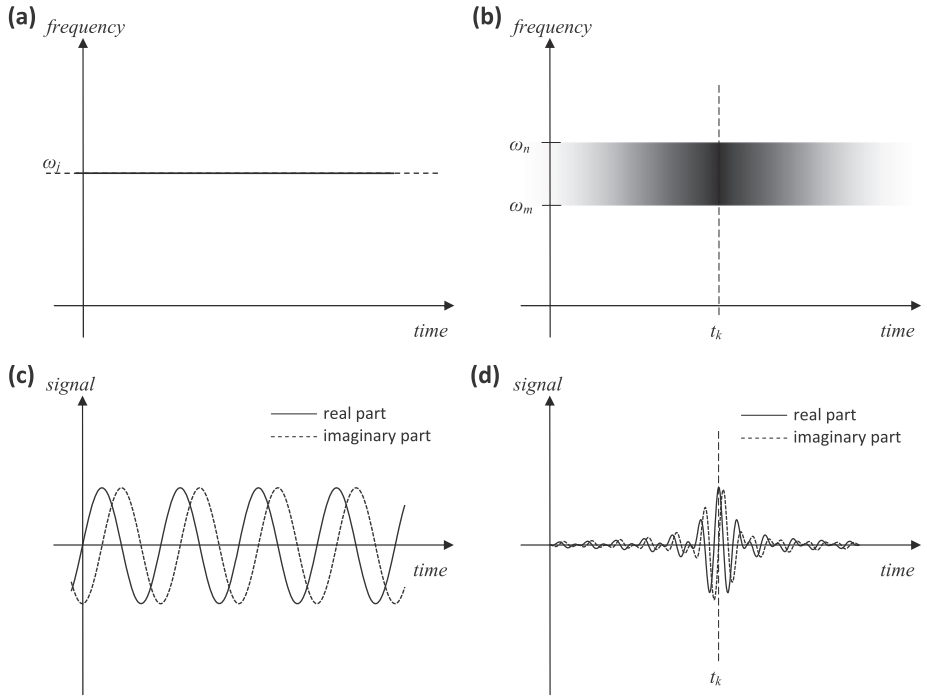

Fig. 2. Single harmonic wave (a and c) versus single wavelet (b and d).

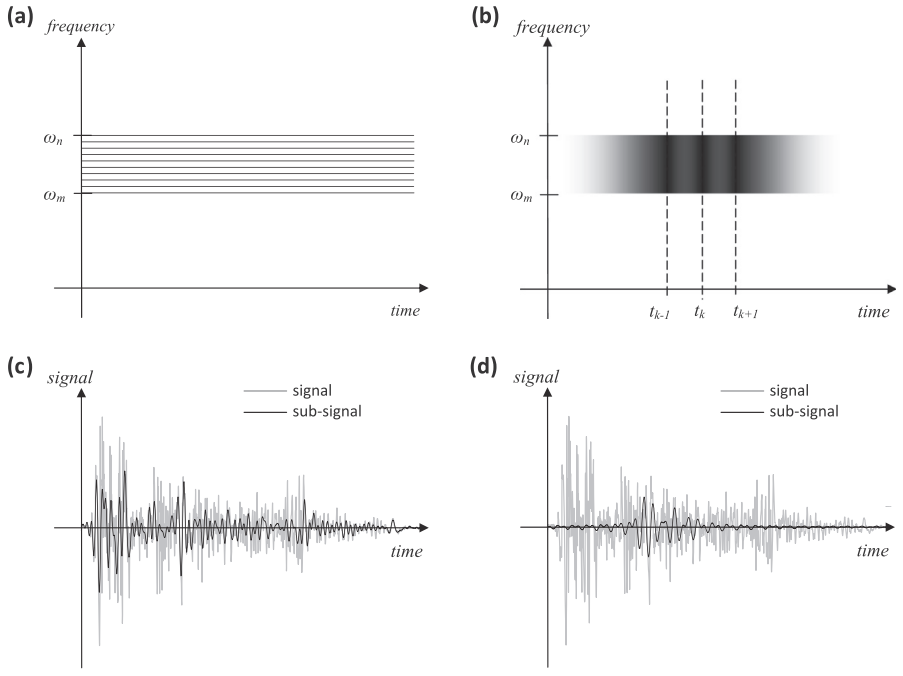

Fig. 3. Sub-signal extraction by FT (a and c) versus HWT (b and d).

a recorded accelerogram (grey lines in the bottom graphs). In the first case (graphs in the left column of Fig. 3), i.e. when a FT-based approach is adopted, more harmonic waves must be taken within the frequency band $[\omega_m, \omega_n[$ (Fig. 3(a)), and it is not possible to localise their contribution in the time axis, as shown with the extracted sub-signal (thick line) in Fig. 3(c). In the second case, on the contrary (graphs in the right column of Fig. 3), the HWT allows retaining in the sub-signal just the wavelets at the given level $\{m, n\}$ which are centred in a prescribed time interval, therefore achieving a joint localisation in both time and frequency domains (see Fig. 3(d)).

3. Spectral matching procedure

The proposed method of spectral matching aims to use a well established and transparent tool of signal analysis and processing, such as the HWT summarised in the previous section, to iteratively introduce localised time–frequency modifications in a given accelerogram, until the updated response spectrum is fitted within the interval bounded by -10% and $+30\%$ of the target EDS. The lower bound (identified in the following with a superscripted flat sign $\flat$) relates to a design prescription and, in this instance, has been chosen in agreement with Eurocode 8 [27]. The upper bound

(identified with a superscripted sharp sign ♯) limits the peaks of the EDS that could otherwise lead to an overly conservative design; the value of +30% has been chosen after testing the iterative algorithm, which has shown the need of this relatively wide interval to limit the number of iterations. The assumed compatibility interval can be reduced, e.g. to ±5%, but this would inevitably increase the number of iterations needed to fit the EDS and would also limit the variability of the resulting spectrum-compatible accelerograms, which on the contrary has to be allowed for (e.g. Ref. [28]). As a matter of fact, given the inherent uncertainties in the seismic action, having a higher level of variability with the ERS of the modified record can be deemed as a way to account for these uncertainties, although further studies would be required to identify the optimal definition of the compatibility interval.

As illustrated in the following, the proposed method attempts to minimise the impact of the modifications done on the recorded accelerogram by exploiting the idea that, once the maximum response value has been reached by a SDoF oscillator of a given natural period T_j, what happens thereafter does not affect (in a linear elastic analysis) the response spectrum ordinate, and hence there is no reason to modify that part of the record. In order to achieve this, the instant τ_j at which the maximum response is attained must be identified, allowing adjustment of the record in the vicinity of this time instant. Noticeably, while FT-based methods bring corrections localised in frequency domain only, the proposed HWT-based method applies modifications localised in both time and frequency domains.

3.1. Derivation of the matching algorithm

For derivation purposes, let us consider the seismic vibration of a linear SDoF oscillator with natural period T_j. The equation of motion reads:

$$\ddot{u}_j(t) + 2\zeta_0\,\omega_j\,\dot{u}_j(t) + \omega_j^2\,u_j(t) = -f(t), \tag{13}$$

where $u_j(t)$ is the displacement of the oscillator; $\omega_j = 2\pi/T_j$ is the natural circular frequency of vibration; $f(t)$ is the time history of ground acceleration; the over-dot means derivative with respect to time t; and $\zeta_0 = 0.05$ is the reference value of the viscous damping ratio. If Eq. (13) is integrated (with initial conditions set to zero) for a number N_T of natural periods T_j, the ERS in terms of pseudo-acceleration (PA) can be defined as:

$$S_{\mathrm{PA}}(T_j) = \omega_j^2 \max_{0\leqslant\ell\leqslant N_t}\{|u_j(t_\ell)|\}, \tag{14}$$

where $t_\ell = \ell\Delta t$ is the ℓth of the $N_t = t_f/\Delta t$ discrete time instants at which the seismic response of each oscillator is computed, Δt being the sampling interval. We can also define the ToM (time-of-maximum) spectrum, which collects the τ_j time instants at which, for different periods of vibration T_j, the peak seismic response is attained:

$$S_{\mathrm{ToM}}(T_j) = \tau_j \text{ such that } S_{\mathrm{PA}}(T_j) = \omega_j^2\,|u_j(\tau_j)|. \tag{15}$$

Both ERS and ToM spectra are calculated for the N_T periods of vibration associated with the relevant discrete frequencies of the signal: that is, for $T_j = 2\pi/(j\Delta\omega)$, where $\Delta\omega = 2\pi/t_f$ and the index $j \in [1, N_t/2]$ takes all the values strictly needed to cover the range where the compatibility is of interest, i.e. $0.1 \leqslant T_j \leqslant 4.0\,\mathrm{s}$ in this study. This leads to the condition $j_{\min} = \mathrm{int}(0.25\,t_f) \leqslant j \leqslant j_{\max} = \mathrm{int}(10\,t_f)$, where t_f is expressed in seconds and $\mathrm{int}(\cdot)$ is the integer function, which returns the integer part of the argument within parentheses.

The first step of the proposed matching procedure is to scale the natural accelerogram by a convenient factor [29] given by:

$$\alpha^{(0)} = \underset{\alpha>0}{\mathrm{argmin}}\left\{\sqrt{\frac{1}{j_{\max}-j_{\min}}\sum_{j=j_{\min}}^{j_{\max}}\left(\frac{\alpha S_{\mathrm{PA}}^{(0)}(T_j) - S_{\mathrm{ED}}(T_j)}{S_{\mathrm{ED}}(T_j)}\right)^2}\right\}, \tag{16}$$

which leads to minimise the root mean square (RMS) discrepancy between EDS given by the code, S_{ED}, and the ERS of the selected accelerogram, S_{PA}, at the 0th iteration. The method then proceeds with iterations until the spectrum compatibility is met. The generic rth iteration requires the following five steps:

1. The current/target spectral ratios are computed:

$$R_j^{(r)} = \min\left\{\frac{S_{\mathrm{PA}}^{(r)}(T_j)}{S_{\mathrm{ED}}^{\flat}(T_j)}, \frac{S_{\mathrm{ED}}^{\sharp}(T_j)}{S_{\mathrm{PA}}^{(r)}(T_j)}\right\}, \tag{17}$$

where $S_{\mathrm{ED}}^{\flat}(T_j)$ and $S_{\mathrm{ED}}^{\sharp}(T_j)$ are the lower and upper bounds of the assumed compatibility zone, respectively, and $S_{\mathrm{PA}}^{(r)}(T_j)$ is the ERS related to the signal at the current rth iteration. If $R_j^{(r)} \geqslant 1$, then the spectral matching is achieved for all the periods of interest and no further iterations are needed; if not, the worst point in terms of compatibility with the target EDS is sought as:

$$j_{\mathrm{worst}} = \underset{j_{\min}\leqslant j\leqslant j_{\max}}{\mathrm{argmin}}\{R_j^{(r)}\}. \tag{18}$$

In this way the rth iteration will be focused on the point having the largest relative distance from the bounded zone, and the intervention in the rth iteration will be localised in the time domain around $t = \tau^{(r)} = \tau_{j_{\mathrm{worst}}}$ and in frequency domain around $\omega = \Omega^{(r)} = \omega_{j_{\mathrm{worst}}}$.

2. The frequency band $[\omega_m^{(r)}, \omega_n^{(r)}[$ to be modified in the current iteration is defined by means of its central frequency $\Omega^{(r)}$ and its bandwidth $B^{(r)}$, given by:

$$B^{(r)} = (N_\omega^{(r)} - 1)\,\Delta\omega, \tag{19}$$

and therefore:

$$\omega_m^{(r)} = \Omega^{(r)} - B^{(r)}/2; \tag{20a}$$

$$\omega_n^{(r)} = \omega_m^{(r)} + B^{(r)}, \tag{20b}$$

subjected to:

$$N_\omega^{(r)} \geqslant N_{\omega,\min} \tag{21a}$$

and:

$$\frac{2\pi}{\omega_m^{(r)}} - \frac{2\pi}{\omega_n^{(r)}} \geqslant \Delta T_{\min}, \tag{21b}$$

in which $N_{\omega,\min}$ is the minimum number of discrete frequencies belonging to the selected bandwidth, while $\Delta T_{\min}$ is the minimum size of the bandwidth in terms of natural periods. These two parameters have to be chosen properly in order to improve the effectiveness of the iterative scheme (more details are offered in the following).

3. The HWT coefficients $\hat{a}^{(r)}_{\{m^{(r)},n^{(r)}\},k}$ are calculated by a discrete convolution of the signal $f^{(r)}(t)$ with the modifying band wavelets $\hat{\psi}_{\{m^{(r)},n^{(r)}\},k}(t/t_f)$:

$$\hat{a}^{(r)}_{\{m^{(r)},n^{(r)}\},k} = \sum_{\ell=0}^{N_t} f_\ell^{(r)}\,\hat{\psi}_{\{m^{(r)},n^{(r)}\},k}\left(\frac{t_\ell}{t_f}\right), \tag{22}$$

with $k = 1,\ldots,(n-m)$ and $f_\ell^{(r)} = f^{(r)}(t_\ell)$; then an expedient time-localised sub-signal for the frequency-localised worst case $j = j_{\mathrm{worst}}$ is obtained as:

$$\tilde{f}^{(r)}(t) = 2\,\mathrm{Re}\left\{\sum_{k=k_1^{(r)}}^{k_2^{(r)}} \hat{a}^{(r)}_{\{m^{(r)},n^{(r)}\},k}\;\hat{\psi}_{\{m^{(r)},n^{(r)}\},k}\left(\frac{t}{t_f}\right)\right\}, \tag{23}$$

which is a summation of the wavelets weighted with the HWT coefficients $\hat{a}^{(r)}_{\{m^{(r)},n^{(r)}\},k}$, with the index k taking all the values within the interval $[k_1^{(r)}, k_2^{(r)}]$. According to the reconstruction formula of Eq. (12), $k_2^{(r)} \leqslant n^{(r)} - m^{(r)}$ and $k_1^{(r)} \geqslant 0$; in order to localise the sub-signal where needed along the time axis, these values can be evaluated as:

$$k_2^{(r)} = \mathrm{int}\left\{\frac{\tau^{(r)}}{t_f}(n^{(r)} - m^{(r)})\right\} + 1; \tag{24}$$

$$k_1^{(r)} = k_2^{(r)} - \mathrm{int}\left\{\frac{\Delta\tau^{(r)}}{t_f}(n^{(r)} - m^{(r)})\right\} + 1; \tag{25}$$

meaning that (see Fig. 4) the time interval in which the bulk of the modification occurs ideally ends at the k-index after the time of maximum response $\tau^{(r)} = S_{\mathrm{ToM}}(2\pi/\Omega^{(r)})$, and begins at the k-index before it, minus the transient duration $\Delta\tau^{(r)} = 3\left(\zeta_0\,\Omega^{(r)}\right)^{-1}$, which is conventionally assumed in this study as the time interval needed to reduce by 95% the free vibration of a SDoF oscillator with natural circular frequency $\Omega^{(r)}$.

4. The displacement response $\tilde{u}^{(r)}_{j_{\mathrm{worst}}}(t)$ can be evaluated by solving the differential equation:

$$\ddot{\tilde{u}}^{(r)}_j(t) + 2\,\zeta_0\,\omega_j\,\dot{\tilde{u}}^{(r)}_j(t) + \omega_j^2\,\tilde{u}^{(r)}_j(t) = -\tilde{f}^{(r)}(t), \tag{26}$$

which for $j = j_{\mathrm{worst}}$ rules the seismic vibration of a SDoF linear oscillator having the natural circular frequency $\Omega^{(r)}$ and subjected to the sub-signal $\tilde{f}^{(r)}(t)$ only. Then a product function is defined by:

$$P^{(r)}_\ell = u^{(r)}_{j_{\mathrm{worst}},\ell}\;\tilde{u}^{(r)}_{j_{\mathrm{worst}},\ell}, \tag{27}$$

whose maximum value is sought as:

$$\ell_{\max} = \underset{0\leqslant\ell\leqslant N_t}{\arg\max}\{P^{(r)}_\ell\}, \tag{28}$$

which therefore delivers the value $\ell_{\max}$ for which the product function between the response to the current signal, $f^{(r)}(t)$, and the response to the current sub-signal, $\tilde{f}^{(r)}(t)$ takes the (positive) maximum.

5. The correction factor for the rth iteration is calculated as:

$$\alpha^{(r)} = \frac{D^{(r)} - u^{(r)}_{j_{\mathrm{worst}},\ell_{\max}}}{\tilde{u}^{(r)}_{j_{\mathrm{worst}},\ell_{\max}}}, \tag{29}$$

where the indexes $j = j_{\mathrm{worst}}$ and $\ell = \ell_{\max}$ localise the correction in the frequency domain and in the time domain, respectively, while the reference spectral displacement $D^{(r)}$ at the rth iteration is given by:

$$D^{(r)} = \left(\frac{T^{(r)}}{2\pi}\right)^2 A^{(r)}_{\mathrm{T}}, \tag{30}$$

in which $T^{(r)} = 2\pi/(\Omega^{(r)})$ and $A^{(r)}_{\mathrm{T}}$ is the target acceleration at the rth iteration. If the current elastic response spectrum underestimates the design value given by the code for the worst case, i.e. if $S^{(r)}_{\mathrm{PA}}\left(T^{(r)}\right) < S_{\mathrm{ED}}\left(T^{(r)}\right)$, then the target acceleration is assumed to be $A^{(r)}_{\mathrm{T}} = 1.05\,S^{\flat}_{\mathrm{ED}}\left(T^{(r)}\right)$, which is 5% higher that the lower bound of the compatibility interval; on the contrary, if the opposite happens, i.e. if $S^{(r)}_{\mathrm{PA}}\left(T^{(r)}\right) > S_{\mathrm{ED}}\left(T^{(r)}\right)$, then the target acceleration is taken as $A^{(r)}_{\mathrm{T}} = 0.95\,S^{\sharp}_{\mathrm{ED}}\left(T^{(r)}\right)$, which is 5% less that the upper bound of the compatibility interval These ±5% coefficients have been simply introduced to avoid targeting the modifications to meet exactly the boundaries of the compatibility interval, which may cause the need of further corrections in the following iterations.

6. The accelerogram is modified as:

$$f^{(r+1)}(t) = f^{(r)}(t) + \alpha^{(r)}\,\tilde{f}^{(r)}(t), \tag{31}$$

and then the next iteration can begin.

Noticeably, the last step is based on the superposition principle: that is, the seismic response $u^{(r+1)}_j(t)$ of the jth SDoF oscillator at the $(r+1)$th iteration is thought as given by the superposition of the responses to the two separate inputs, namely the accelerogram at the previous iteration, $f^{(r)}(t)$, and its time–frequency jointly-localised component, $\tilde{f}^{(r)}(t)$, multiplied by the coefficient $\alpha^{(r)}$. Since the latter quantity has been related to the spectral value to be adjusted, in both time and frequency domains, it is likely that the best correlation between the two separate responses is achieved at the instant of maximum product, $t_{\ell_{\max}}$. Interestingly, while up-modifications (when S_{PA} is increased) always work, down-modifications sometimes fail to reduce the spectral values S_{PA} to the desired level. In fact, while the response peak affecting the spectral value at the rth iteration is reduced, there could be another peak located somewhere else on the time axis, which may require a further iteration. Nonetheless, by numerical testing on a range of different recorded signals and target spectra, we have found a satisfactory rate of success of about 95% for the down-modifications, which in turn ensures the overall convergence of the proposed procedure of spectral matching.

3.2. Discussion

As highlighted in the previous subsection, the proposed algorithm is able to adjust the ordinates of the ERS of a recorded accelerogram by means of iterative modifications localised both in the time and in frequency domain. Nevertheless, fitting the modified ERS $S^{(r)}_{\mathrm{PA}}(T)$ within the bounded interval of compatibility $\left[S^{\flat}_{\mathrm{ED}}(T), S^{\sharp}_{\mathrm{ED}}(T)\right]$ over the full range of periods of vibration which are of interest for design purposes does not follow trivially, especially because this should be achieved with a reasonably small number of iterations (ideally, less than fifty). The algorithm does not cap the value of the $\alpha^{(r)}$ coefficients, therefore a final check on the additional energy introduced in the signal should be performed to ensure that the corrective terms do not distort excessively the original record.

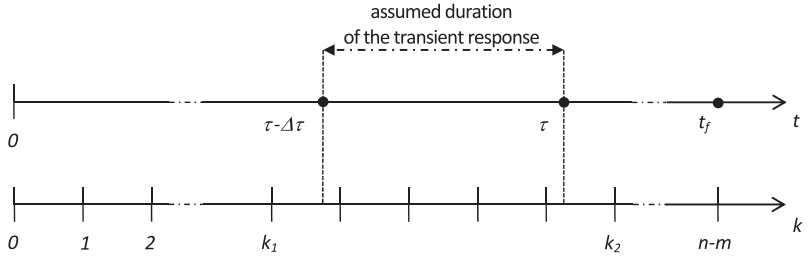

Fig. 4. k_1, k_2 definition.

The main reason for these difficulties is that for $\zeta_0 = 0.05$ (reference value of the viscous damping ratio), the dispersion of the dynamic amplification function around the natural frequency of the target SDoF oscillator is not sharp enough to avoid that the adjustment brought to the chosen value on the spectrum does not affect significantly also the values in its proximity. Moreover, despite the localisation capabilities of harmonic wavelets, these functions are centred on discrete points, which usually do not match perfectly with the points where the original signal needs to be modified.

As a result, stalling in convergence is possible in principle, with a sort of ping-pong effect, i.e. the algorithm may spend several iterations attempting to fit the spectrum in a certain range. However, this issue can be overcome with a proper choice of the parameters $N_{\omega,\min}$ and $\Delta T_{\min}$, which rule the size of the band subjected to modification (see step (2) above). It should be noted that these two parameters affect different ranges: that is, $N_{\omega,\min}$ limits the bandwidth in the range of long periods of vibration, while $\Delta T_{\min}$ affects the short periods. In all the analyses reported in the next subsection, we have used $N_{\omega,\min} = 9$ and values of the parameter $\Delta T_{\min}$ between 0.05 and 0.2s, as our extensive numerical campaign has clearly shown that this choice optimises the convergence rate, and allows to achieve the spectral matching without exploiting more complicated schemes, e.g. considering in step (1) the worst band rather then the worst frequency.

4. Numerical examples

In order to assess the effectiveness of the proposed procedure, several recorded accelerograms have been studied to cover

Table 1
Cases of study.

Earthquake	Site/component	Δt (s)	t_f (s)	M_w	Depth/distance (km)	PGA (g)
Imperial Valley 1940	El Centro/N-S	0.010	40	7.0	8.80/6.09	0.258
Erzincan 1992	Erzincan/E-W	0.005	20	6.7	27.00/0.00	0.495
Irpinia 1980	Calitri/E-W	0.005	80	6.9	15.00/13.30	0.175

Table 2
Matching details.

Record	Target EDS	α_0	RMS_0	FT		HWT	
				$\Delta\mathcal{E}$ (%)	RMS_f	$\Delta\mathcal{E}$ (%)	RMS_f
El Centro 1940	B (best)	1.361	0.162	+36.4	0.132	+16.9	0.152
Erzincan 1992	D (best)	1.106	0.237	+107.1	0.137	+46.3	0.140
Irpinia 1980	A (worst)	1.017	0.208	+201.9	0.157	+68.7	0.136

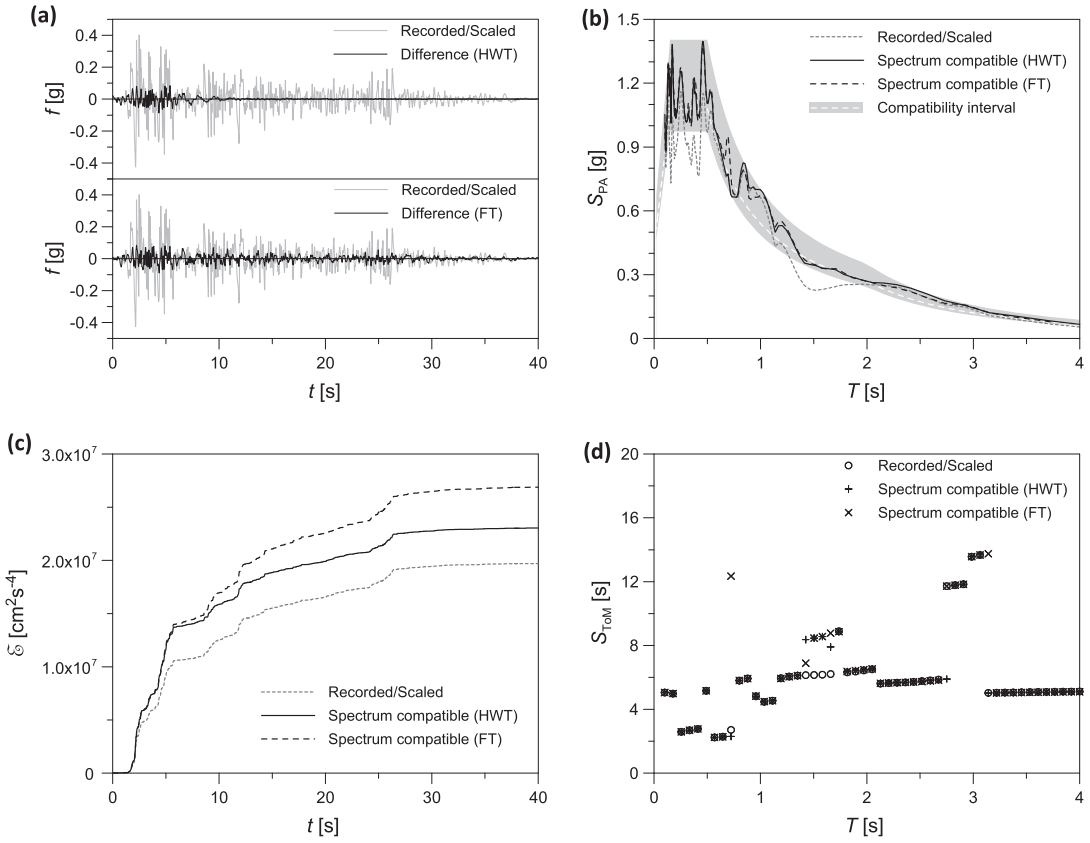

Fig. 5. El Centro 1940 matching the EC8 soil-type B EDS: (a) comparison between the modifications introduced (difference) by the FT and the HWT methods; (b) EDS and compatibility interval; (c) cumulative energy; (d) time of maximum (ToM) spectra.

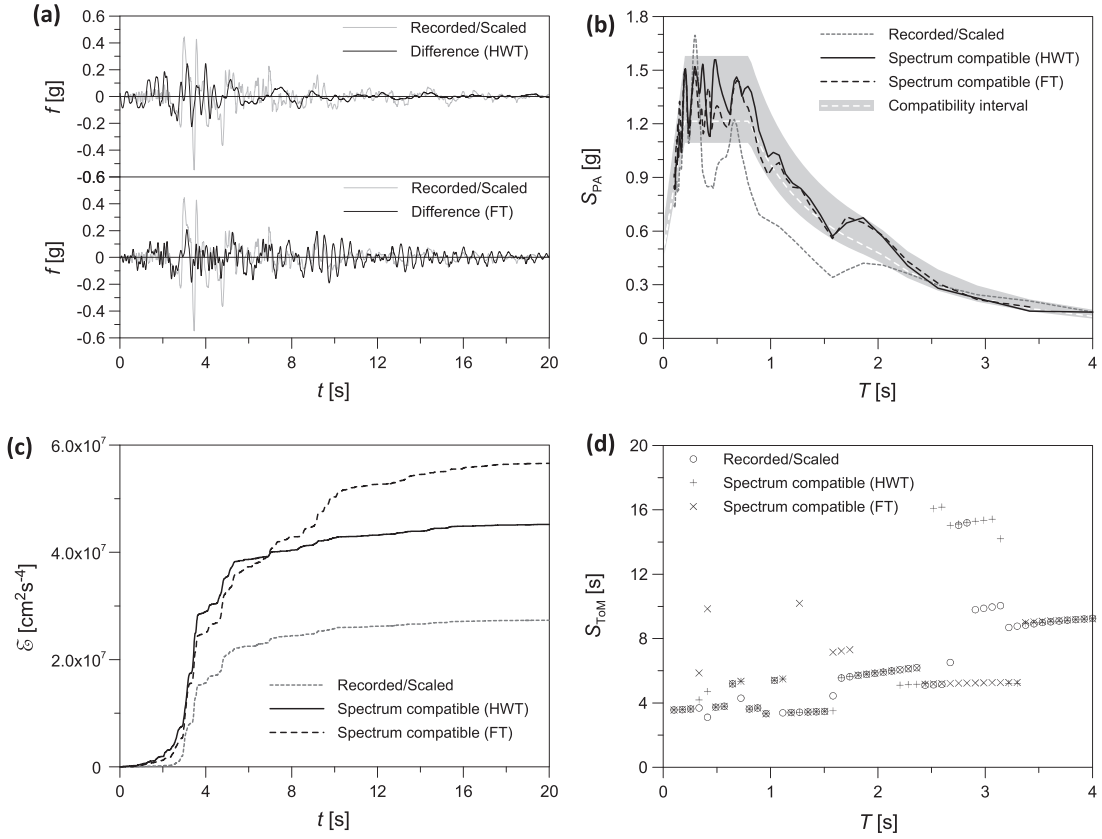

Fig. 6. Erzincan 1992 matching the EC8 soil-type D EDS (best initial matching).

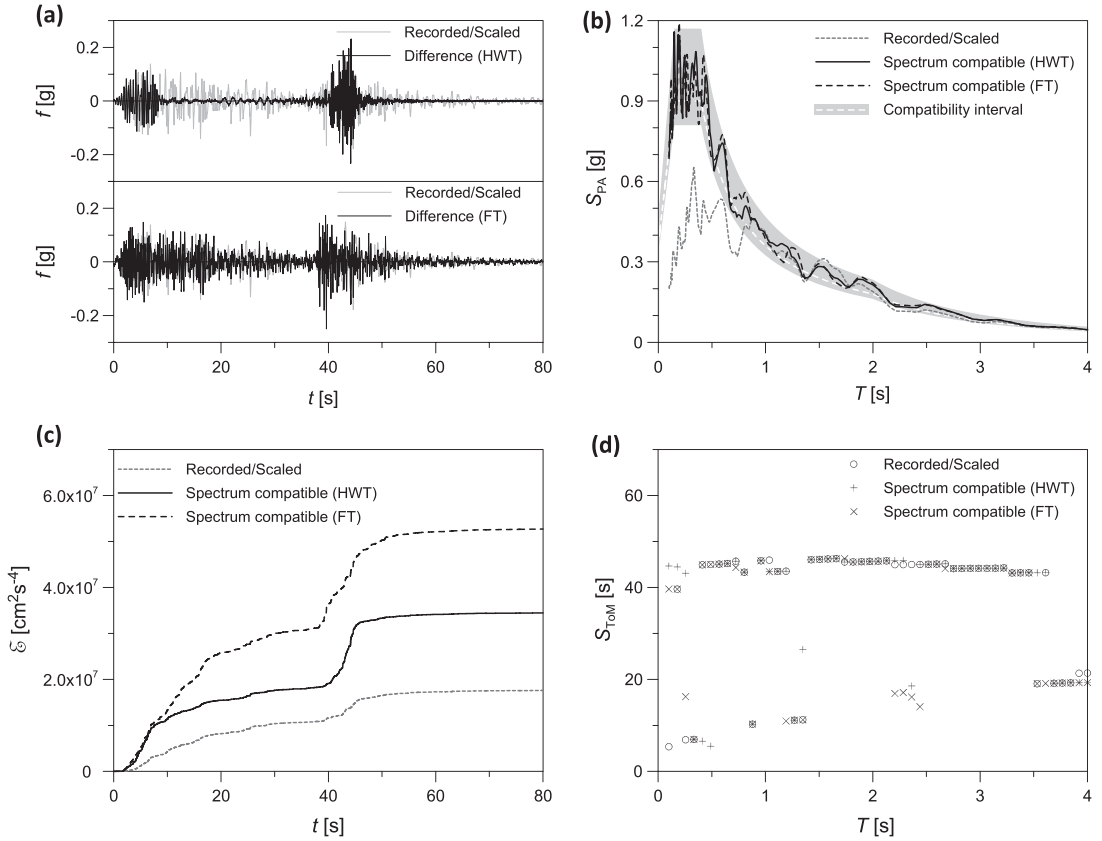

Fig. 7. Irpinia 1980 matching the EC8 soil-type A (worst initial matching).

different design scenarios. The HWT-based method has been used to match these records within the chosen compatibility interval for the Eurocode (EC8) spectral shapes. The peak ground acceleration (PGA) of 0.36 g has been assumed, and both the best and the worst initial matching in terms of RMS discrepancy with the target EDS (see Eq. (16)) has been considered. For comparison purposes, an FT-based method has been also implemented by using the same algorithm described above, modified in step (3) letting $k_1 = 0, k_2 = N_t/(n-m)$, which means that all k-indexed coefficients of the wavelet train in the selected frequency band are used, and hence no time localisation is exploited (therefore highlighting the improved performance of the HWT, which allows for such localisation on the time domain). Importantly, this FT-based method is equivalent to scale uniformly, over the whole duration of the recorded accelerogram, the sub-signal associated with the frequency band $[\omega_m^{(r)}, \omega_n^{(r)}[$ in the rth iteration, similarly to what happens in the matching procedures used in Refs. [4,15], which do not exploit the ToM spectrum. For this reason, the FT-based method has been adopted in our investigations as a reference procedure to highlight the improved performance of the proposed HWT-based method in comparison with existing methods of spectral matching.

The results are presented for three selected accelerograms (El Centro 1940; Erzincan 1992; Irpinia 1980), whose main characteristics (sampling time step Δt, duration t_f, moment magnitude M_w, focal depth, Joyner-Boore distance and the PGA) are listed in Table 1. Table 2 displays the additional energy $\Delta\mathcal{E}$ required to achieve the spectral compatibility (with both FT and HWT procedures), along with the initial scaling factor α_0 (see Eq. (16)) and the values of the RMS discrepancy with the target EDS at both initial (0) and final (f) stages. Similar results have been consistently obtained for other records [30], which however have been omitted herein for the sake of brevity, as the following three accelerograms appear to cover a range of realistic design situations:

- The El Centro 1940 accelerogram has been considered because its ERS closely resembles the EC8 EDS shapes (see Fig. 5(b)). The best initial matching (Eq. (16)) is with the EC8 soil-type B (see Table 2), and the advantage of the proposed HWT-based procedure over the FT-based approach is apparent considering that the increase in the total energy due to the modification ($\Delta\mathcal{E}$) is more than halved (see Fig. 5(c)).
- The Erzincan 1992 accelerogram has been chosen as an example of near-fault record, characterised by an impulse in terms of ground velocity and displacement (partially visible in the time history of the ground acceleration shown within Fig. 6(a)), and also in this case the best initial RMS matching (with the EC8 soil-type D, see Table 2) has been considered.
- Finally, the Irpinia 1980 record has been selected because of its peculiar nature showing a double intense phase (see Fig. 7(a)), due to a two-stage fault rupture. The results are shown in this case for the worst matching spectral shape (A), therefore providing an example of the effectiveness of the procedure in a more challenging scenario.

In all the three numerical examples, the performance of the proposed HWT-based correction, due to its joint localisation in time and frequency, is better than the FT-based correction, for which the increase in the cumulative energy of the signal, $\Delta\mathcal{E}$, is doubled (as apparent in all the bottom-left sub-graphs (c) of Figs. 5–7), meaning that more modifications are required to achieve the spectral compatibility, and hence the original characteristics of the accelerograms are more heavily affected. This clearly emerges also from the top-left sub-graphs (a) of Figs. 5–7, where the solid black lines show the corrections applied to the original record, which are much more localised in the HWT-based procedure, while they are spread over the overall duration when the FT is adopted. Top-right sub-graphs (b) show that both HWT and FT allow achieving the desired compatibility, even if the original ERS and the target EDS supplied by the building code have very different shapes. This is particularly evident within Fig. 7(b), as the spectral compatibility of the Irpinia 1980 accelerogram with the EC8 soil-type A has required corrections having about the same amplitude as the original record (see Fig. 7(a)). Sub-graphs (d) show the ToM spectra (whose exploitation is peculiar to the proposed method), and once again the HWT performs better since the FT tends to disturb more the original distribution of the time instants where the response maxima are attained.

5. Concluding remarks

In this study, the HWT (harmonic wavelet transform) was found to be a very powerful tool for dealing with seismic signals and their inherent non-stationarity, both in terms of amplitude and frequency content, which in turn may play a crucial role for the purposes of analysis and design of earthquake-resistant structures. This paper presents a deterministic modification method, aimed at matching the ERS (elastic response spectrum) of a given accelerogram to a target EDS (elastic design spectrum), while a future paper will focus on a stochastic generation procedure, able to randomise a parent signal to get an arbitrary number of samples with similar non-stationary features.

It has been shown that the proposed spectral matching method, working in an iterative way, operates adjustments in the original signal, which are localised in both time and frequency domains, and for this reason is able to achieve the required spectral compatibility with limited modifications in terms of additional energy content. This was obtained by using two complementary earthquake spectra, in terms of peak accelerations (S_{PA}) and times of maximum response (S_{ToM}), to determine the corrective term in each iteration. Extensive numerical investigations have demonstrated the excellent performance of the proposed method, particularly in comparison with a traditional approach based on the Fourier transform (FT), whose results are equivalent to those that other investigators have obtained in the past using the wavelets without information drawn from the S_{ToM} spectrum.

A possible source of criticism for the proposed approach could be associated with the conventional (and rather unrealistic) nature of the EDS prescribed by seismic codes. As a matter of fact, the EDS is an synthetic representation of the hazard related to different seismic events at a given site, rather than a regularised ERS for a single design scenario. For instance, the ordinates of the EDS for low periods account for relatively less intense but nearer events, while those for long periods are mainly influenced by the possibility of having stronger but farther earthquakes [17]. Indeed, a natural accelerogram generally does not possess enough energy as necessary to match the EDS for all the periods of vibration, particularly because of the filtering effects of the soil deposit at a given site, while with the proposed approach any lack or excess of energy in some sub-signals of the original record is adjusted with modifications which, however, inevitably distort the original accelerogram and (usually) tend to increase the total energy of the input. Nevertheless, the availability of such a modified accelerogram, which shows a code-compliant ERS but yet brings as much realistic features as possible, can be very useful in a number of practical design situations, as long as the resulting record is consistent with the given hazard scenario. In order to further widen the applicability of the proposed HWT-based method, two main developments could be considered in the future: first, the multi-component extension, so to pursue the spectral matching with the principal components of the recorded event; second, the multi-record

extension, so to modify not a single record, but a suite of natural records to achieve the on-average spectral compatibility, which will then reduce the amount of modifications needed to meet the target and the additional energy. Moreover, further analyses will be required in the future to ascertain the effects of the HWT-based modifications on the seismic response of various non-linear structures.

Acknowledgements

This work has been partially supported by the EPSRC (the UK Engineering and Physical Sciences Research Council), under the "2010 Grant Balances" EP/J014400/1.

References

[1] Katsanos EI, Sextos AG, Manolis GD. Selection of earthquake ground motion records: a state-of-the-art review from a structural engineering perspective. Soil Dynam Earthq Eng 2010;30(4):157–69.
[2] Sabetta F, Pugliese A. Estimation of response spectra and simulation of nonstationary earthquake ground motions. Bull Seismol Soc Am 1996;86(2):337–52.
[3] Rezaeian S, Der Kiureghian A. Simulation of synthetic ground motions for specified earthquake and site characteristics. Earthq Eng Struct Dynam 2010;39(10):1155–80.
[4] Mukherjee S, Gupta K. Wavelet based generation of spectrum compatible time-histories. Soil Dynam Earthq Eng 2002;22(9–12):799–804.
[5] Suárez LE, Montejo LA. Generation of artificial earthquakes via the wavelet transform. Int J Solids Struct 2005;42(21–22):5905–19.
[6] Hancock J, Watson-Lamprey J, Abrahamson NA, Bommer JJ, Markatis A, McCoy E, et al. An improved method of matching response spectra of recorded earthquake ground motion using wavelets. J Earthq Eng 2006;10(Suppl. 1):67–89.
[7] Das S, Gupta VK. Wavelet-based simulation of spectrum-compatible aftershock accelerograms. Earthq Eng Struct Dynam 2008;37(11):1333–48.
[8] Yazdani A, Takada T. Wavelet based generation of energy- and spectrum-compatible earthquake time histories. Comput-Aid Civil Infrastruct Eng 2009;24(4):623–30.
[9] Cacciola P. A stochastic approach for generating spectrum compatible fully nonstationary earthquakes. Comput Struct 2010;88(15–16):889–901.
[10] Zerva A. Seismic source mechanisms and ground motion models. Probab Eng Mech 1988;3(2):64–74.
[11] Lam N, Wilson J, Hutchinson G. Generation of synthetic earthquake accelerograms using seismological modelling: a review. J Earthq Eng 2000;4(3):321–54.
[12] Cacciola P. Stochastic ground motion modelling for the seismic analysis of structures: a review. In: Topping BV, editor. Computational technology review 4. Stirling (UK): Saxe-Coburg; 2011. p. 65–91. http://dx.doi.org/10.4203/ctr.4.3.
[13] Gasparini D, Vanmarke E. Simulated earthquake motions compatible with prescribed response spectra. Publication no. r76-4, tech. rep., Massachusetts Institute of Technology (MIT), Department of Civil Engineering; 1976.
[14] Shinozuka M, Deodatis G. Stochastic process models for earthquake ground motion. Probab Eng Mech 1988;3(3):114–23.
[15] Giaralis A, Spanos PD. Wavelet-based response spectrum compatible synthesis of accelerograms – eurocode application (EC8). Soil Dynam Earthq Eng 2009;29(1):219–35.
[16] Italian Ministry of Infrastructures, Norme Tecniche per le Costruzioni; 2008 [In Italian].
[17] Bommer JJ, Acevedo AB. The use of real earthquake accelerograms as input to dynamic analysis. J Earthq Eng 2004;8(Suppl. 1):43–91, 200.
[18] Schwab P, Lestuzzi P. Assessment of the seismic non-linear behavior of ductile structures due to synthetic earthquakes. Bull Earthq Eng 2007;5(1):67–84.
[19] Beck J, Papadimitriou C. Moving resonance in nonlinear response to fully non-stationary stochastic ground motion. Probab Eng Mech 1993;8(3–4):157–67.
[20] Wang J, Fan L, Qian S, Zhou J. Simulations of non-stationary frequency content and its importance to seismic assessment of structures. Earthq Eng Struct Dynam 2002;31(4):993–1005.
[21] Mallat SG. A wavelet tour of signal processing: the sparse way. 3rd ed. Academic Press; 2009.
[22] Spanos PD, Failla G, Politis NP. Wavelets – concepts and applications. In: De Silva CW, editor. Vibration and shock handbook. Boca Raton, FL (USA): CRC Press; 2005. p. 11-1–11-24 [chapter 11].
[23] Cecini D, Palmeri A. Spectrum-compliant accelerograms through harmonic wavelet transform. In: Topping BHV, editor. Proc. of the 11th international conference on computational structures technology, Dubrovnik, Croatia; 2012. Paper no. 285, doi: http://dx.doi.org/10.4203/ccp.99.285.
[24] Tang YY. Wavelet theory approach to pattern recognition. 2nd ed. World Scientific; 2009.
[25] Newland DE. Harmonic wavelet analysis. Proc Ro Soc A 1993;443(1917):203–25.
[26] Newland DE. Harmonic and musical wavelets. Proc Roy Soc A 1994;444(1922):605–20.
[27] European Committee for Standardisation, Eurocode 8: Design of structures for earthquake resistance – Part 1: General rules, seismic actions and rules for buildings; 2004 (EN 1998-1).
[28] Cacciola P, Zentner I. Generation of response-spectrum-compatible artificial earthquake accelerograms with random joint time-frequency distributions. Probab Eng Mech 2012;28:52–8.
[29] Iervolino I, Galasso C, Cosenza E. REXEL: computer aided record selection for code-based seismic structural analysis. Bull Earthq Eng 2010;8(2):339–62.
[30] Cecini D. Generation of seismic signals with stochastic methods, Master's thesis, Sapienza University of Rome; 2011.